International Journal of Engineering Trends and Technology
ISSN: 2231–5381 / https://doi.org/10.14445/22315381/IJETT-V71I9P220

Volume 71 Issue 9, 227-232, September 2023
© 2023 Seventh Sense Research Group®

Original Article

Effect of Temperature on $Ni_{0.5}Cu_{0.15}Zn_{0.3}Fe_{2.05}O_4$ Thinfilm Deposited using Spin Coating Technique

S. Sri Surya Srikanth[1], B. Rajesh Kumar[2]

[1,2]*Department of EECE, GITAM School of Technology, Visakhapatnam, India.*

[1]*Corresponding Author : srisuryasrikanth08@gmail.com*

Received: 08 May 2023 Revised: 29 July 2023 Accepted: 15 August 2023 Published: 03 September 2023

Abstract *- The paper focuses on the spin coating method of $Ni_{0.5}Cu_{0.15}Zn_{0.3}Fe_{2.05}O_4$ thinfilm on Si (100) substrate using deposition and characterisation processes. The films are characterised using XRD, FTIR, FESEM, and EDS techniques. The electrical properties are also investigated. When the temperature is changed from 500 to 800°C, the crystallite dimension changes in the range of 12 nm to 25 nm. The values of ferrite tetrahedral sites (599cm-1) and octahedral sites (500cm-1) were validated by FTIR findings. The sample's nanocrystalline composition was revealed via Scanning Electron Microscopy (SEM). The Primary structure of the sample was decided using Energy Dispersive Spectroscopy (EDS). The sol-gel process is the most straightforward way for depositing NZCF films for improved VOC detection outcomes.*

Keywords *- $Ni_{0.5}Cu_{0.15}Zn_{0.3}Fe_{2.05}O_4$, Sol-gel method, FTIR, XRD, SEM, EDS.*

1. Introduction

Gas sensors play a vital role in various applications like monitoring of the environment, industrial fabrication, safety in the domestic field, and surveillance in public security, which are the points of core reflections for combustible gases and NO_x emissions. The creation of solid-state gas sensors having requires global capability and high performance. Bulk ceramic thick films and thin film oxides have been intensely researched during the past ten years as sensor components for gas sensing [1-4].

In the last decade, it has been based on ferrites excavated in the literature for their high-performance characteristics, such as selectivity and sensitivity, which perform way better than n-type semiconducting oxides. It has been noted that materials having the formula MFe_2O_4 (M = Cu, Cd, Zn, and Ni) are spinel-type oxide semiconductors that are sensitive to reducing and oxidising gases [5-8].

In spinel ferrites, conduction is processed with a transfer of charge carriers at equitable cations detected at octahedral sites. A peculiar benefit of spinel-type ferrites is regulating conductivity and resistance by altering cation composition. In NZC, ferrite fabrication control and composition uniformity are essential for thinfilm deposition [9].

The chemical composition of NZC ferrite thin films alters in response to temperature variations, which leads to non-uniformity in the film composition and magnetic hysteresis parameters. The temperature synthesis of NZC ferrites, when it undergoes a high temperature, yields the vaporisation of primary constituents like non-stoichiometric zinc volatilisation, resulting in Fe^{2+} ions reducing the electrical sensitivity. Thus, a low-temperature synthesis is essential for NZC ferrite thin film, which is commonly prepared using sputtering and PLD techniques. The spin coating method is proposed to ways the chemical homogeneity low calcination temperature, preferably at a lower price. Additionally, it gives the liquid film a benefit that promotes thickness uniformity during the spin-off process [10-16].

In this manuscript, the effect of temperature variations is being studied and developed using the stoichiometric compounds equation.

2. Experimental Details

To generate a NiZnCu ferrite thin film, a sol-gel technique and spin-coating equipment are employed. The precursor for the formation of the first salt is nickel nitrate hexahydrate (Ni $(NO_3)_2.6H_2O$) (Sigma Aldrich, 99.999%), ferric nitrate nanohydrate ($Fe(NO_3)_3 9H_2O$) (Alfa Assar, 99.999%) and zinc hexahydrate (99.999%), $Zn(NO_3)_2 6H_2O$) (AlfaAssar, 99.999%). The four salts listed above persisted in dematerialising in 2-methoxy ethanol to produce mixed findings. Using 2-methoxy ethanol, the solution's concentration was raised to 2 mol/L using 10 ml of the sample. The sample F1 is prepared based on a stoichiometric equation. The solution was agitated for 12 hours before being aged at room temperature for 24 hours to generate the stable precursor used in the subsequent step. The wet films are then produced by spin-coating for 40 seconds at 3500 rpm on Si (100) substrates. The thin films are dehydrated at 120 degrees Celsius for about 5 minutes before being sintered at 200 degrees Celsius for 40 minutes to pyrolyse and remove the organic components. The spin coating,

This is an open access article under the CC BY-NC-ND license (http://creativecommons.org/licenses/by-nc-nd/4.0/)

desiccating, and warming processes were recurred to reach the appropriate film thickness. The as-deposited films were then gradually cooled in the furnace after being annealed in the air for 60 minutes at 600°C to 800°C. The above process is repeated for annealing the films at different temperatures, from 500-800ºC of temperature for 60 minutes. [16-21]

Using SEM [22], the surface morphologies and thickness of the films are characterised on Hitachi S-4800 equipped with an Energy-Dispersive Spectrometer (EDS), a Rigaku D/Max-2400, the phases of the films were characterised using X-ray Diffraction (XRD) with Cu K radiation, while I-V characterisation was performed using specifically built equipment. ABB Bommel FTLA2000 Fourier Transform FTIR equipment and KBr as a mulling agent were used to detect compounds in the 400-4000 cm^{-1} range.

3. Results and Discussion

3.1. XRD

The XRD patterns of $Ni_{0.5}Zn_{0.3}Cu_{0.15}Fe_{2.05}O_4$ (F1) thin films annealed at various temperatures (500, 600, 700, 800ºC for 60 min) are shown in Fig. 1. It is observed that there are a few characteristic peaks of NZCF are present in the XRD patterns. It exhibits the NiZnCu ferrites as the main crystalline phases [23-25]. With increasing annealing temperature, the number of precise similar peaks for cubic spinel ferrite increases, as does the crystallinity of the ferrite thin films. Table1 demonstrates that the lattice parameter falls when the temperature rises from 500oC to 800oC.

Debye Scherrer formula indicates for calculating the particle size of the sample:

$$D=\frac{0.89\lambda}{\beta cos\theta} \quad (1)$$

According to equation 1 indicates that λ=1.504A^0, 2-peak location, D-particle size, FWHM on (311) XRD peak at 2θ.

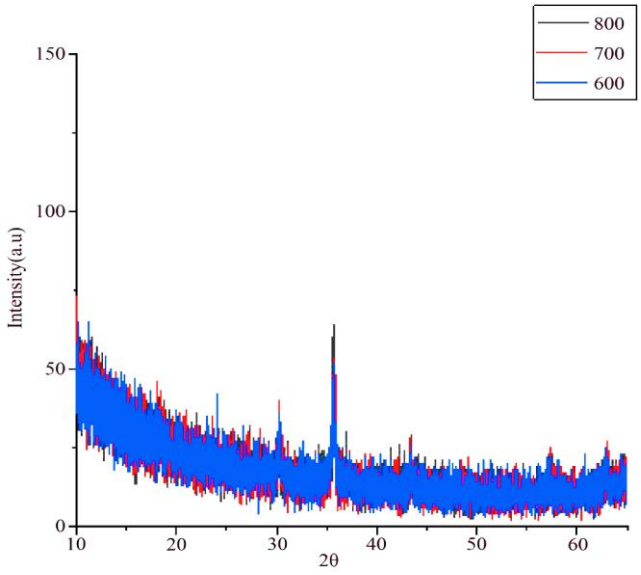

Fig. 1 ThinFilm annealed at 500,600, 700, and 800ºC for XRD patterns

Table 1. XRD Crystallite size and lattice parameters

Sample	Peak Position(2θ)	FWHM	Lattice Constant	D(nm)
600ºC	35.59	0.0055	8.359	12.79
700ºC	35.649	0.0048	8.345	15.38
800ºC	35.661	0.0030	8.343	25.14

Because of the variable grain growth generated by the thermal energy of different annealing temperatures, the determined particles are in the nano range (12nm to 25nm). Table 1 shows that the samples' crystallite dimension and lattice properties are conditioned and annealed.

As the annealing temperature increases, it results in the rise of all medium crystal sample sizes from the above analysis.

3.2. FTIR Investigation

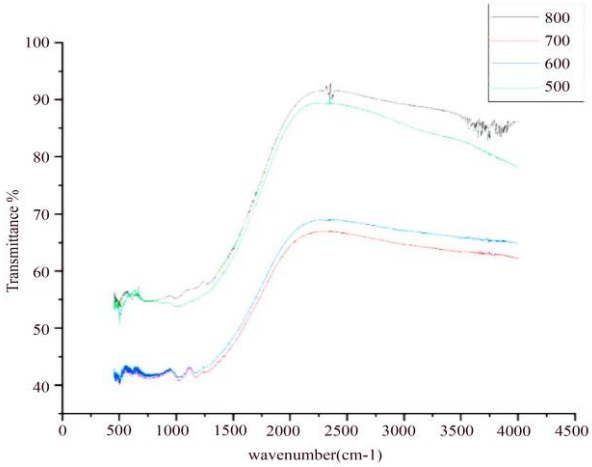

Fig. 2 FTIR spectra of NZC ferrite thinfilm

FTIR spectroscopy is a key instrument for determining ferrite nanoparticle compounds' stretching and bending vibrations. In spinel-type ferrite materials, IR absorption bands have been found [26-29]. Figure 2 illustrates the range of 500-599cm^{-1}. FTIR spectrum of NZC ferrite thin film The absorption spectra confirmed the phase change of the cubic spinel structure and revealed the exact positions of the cations in the crystal structure, along with the oxygen ions and their vibrational states [30].

The structural location and physical properties of ferrite nanoparticles are represented by these IR absorption bands. Based on the nearest neighbor oxygen ions in the geometric arrangement, the metal cations of the ferrite nanoparticles are divided into two sublattices: tetrahedral (A sites) and octahedral (B sites).

Table 2. Variations in temperatures for tetrahedral sites and octahedral sites

Sample	Absorption bands (cm^{-1})	
	υ_t	υ_o
800°C	599	500
700°C	595	499
600°C	508	465
500°C	500	475

The FTIR results demonstrate that the tetrahedral and octahedral sites of the NZC ferrite compound are well-matched with the reported literature [23].

3.3. FESEM

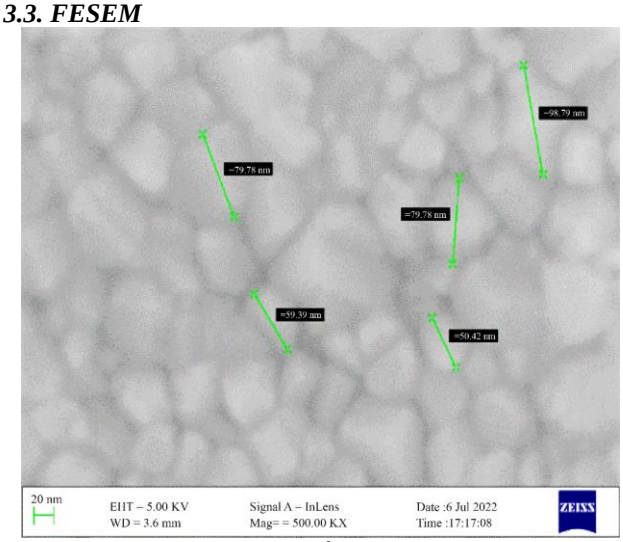

(a) S2 @ 700°C i.e 95nm

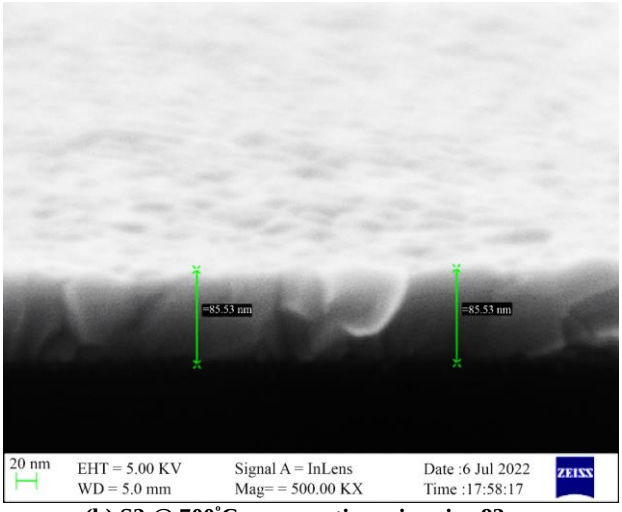

(b) S2 @ 700°C cross-section view, i.e. 83nm

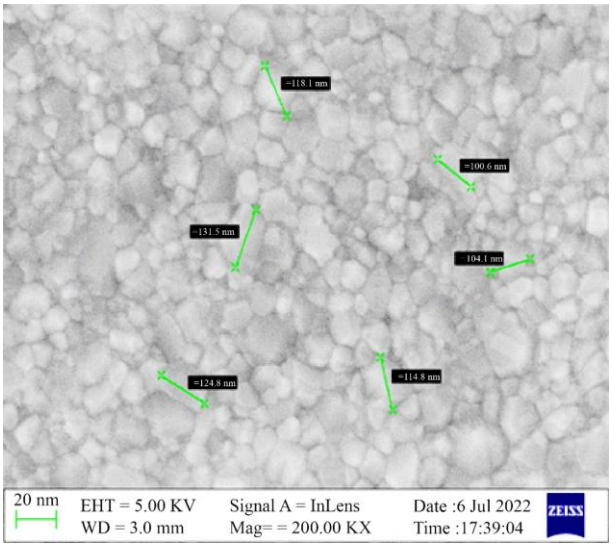

(C) S2 @ 800°C i.e 109nm

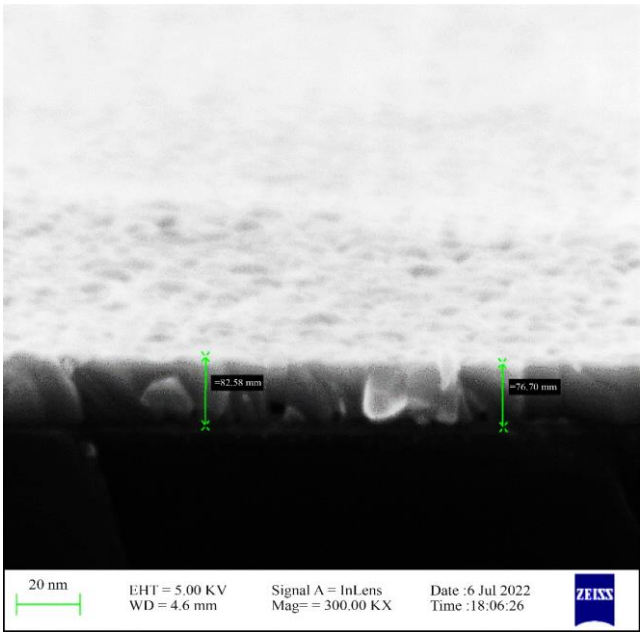

(d) S2 @ 800ºC cross-section view, i.e. 83nm

Fig. 3(a-d) Indicates cross-sectional view and crystallite size for thin films

3.4. Energy-Dispersive X-ray Spectrometer

Energy Dispersive Spectroscopy (EDS) is usually used to examine qualitative materials, although it also gives semi-quantitative data. SEM instrumentation is typically paired with an EDS device to enable chemical investigation of features identified in the SEM display. If spot analysis becomes critical to predictable outcomes, simultaneous SEM and EDS analysis can be advantageous in failure situation analysis. Secondary and backscattered electrons are employed in creating images for morphological studies, and X-rays are used for revealing and quantifying compounds present at distinguishable concentrations. The sample surface conditions alter the threshold for detection in EDS. The lower the detection limit, the smoother the surface. Major and minor elements are identified by EDS with concentrations higher than the wt% (primary) and minor concentrations (concentrations between 1 and 10 wt%).

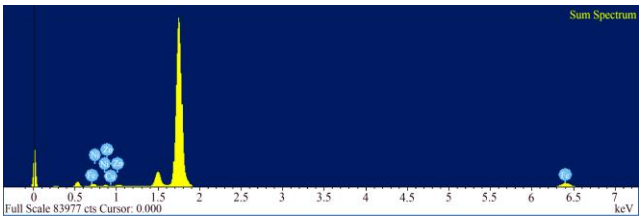

Fig. 4 EDS of Thinfilm

Table 3. Elemental material specification

Element	Weight%	Atomic%
Fe K	61.19	63.50
Ni K	19.21	18.96
Cu K	6.03	5.50
Zn K	13.58	12.04
Totals	100.00	100.00

Table 4. Temperature variations for C-V characterisation

Temperature(°C)	Voltage(volts)	Current(mA)	Resistance(MΩ)
500°C	2	$3.10e^{-6}$	260.276
	3	$2.99e^{-6}$	265.239
	4	$2.15e^{-5}$	276.117
	5	0.001719	290.866
	6	0.002719	300.323
600°C	2	$4.66e^{-10}$	945.341
	3	$4.33e^{-9}$	561.414
	4	$3.35e^{-08}$	355.93
	5	$1.72e^{-7}$	318.70
	6	$6.22e^{-7}$	105.78
700°C	2	$2.02e^{-10}$	2542.0
	3	$1.13e^{-9}$	2654.8
	4	$1.03e^{-9}$	3333.3
	5	$1.01e^{-9}$	4166.6
	6	$0.9e^{-9}$	5454.5
800°C	2	$8.45e^{-12}$	385.218
	3	$2.02e^{-11}$	889.219
	4	$1.02e^{-11}$	1110.11
	5	$0.02e^{-11}$	1250.10
	6	0.00127	1299.00

The cross-sectional SEM image for the sample recovered from the Si (100) substrate and NZC ferrite layer using a sol-gel method is shown in Fig 3(a-d),4. The film has a high packing density and a consistent thickness. To enable chemical investigation of features identified in the SEM display, SEM instrumentation is typically paired with an EDS device. If spot analysis becomes critical to predictable outcomes, simultaneous SEM and EDS analysis can be advantageous in failure situation analysis. The surface morphology of annealed NZCF films shows the grain size. It was observed that the grain size was increased from 89nm to 109nm when the temperature increased from 600 to 800°C, and there was no change in thickness observed with annealing. Fig 4 and Table 3 confirm the material peaks of NZCF films.

3.5. I-V

The sensing performance of the sensor is affected by several operating temperatures and measures the sensor's electrical conductance. The sensor obtains I-V characteristics at 500°C to 800°C, which is listed in Table 4.

From the above table 3, it is evident that the material behaves as a semiconductor compound when the annealing temperature is between 600 and 700°C, which shows the gas sensing property of the material.

4. Conclusion

$Ni_{0.5}Cu_{0.15}Zn_{0.3}Fe_{2.05}O_4$ thinfilm was fabricated on Si (100) substrate using the sol-gel method. The thin film's XRD investigation shows that the sol-gel technique effectively lowers the crystallisation temperature. FTIR results confirm the absorption bands of the material.

It is observed from FESEM results that the grain size increases from 12nm to 25nm when the annealing temperature increases from 600 to 800°C. The resistance change observed using I-V confirms the material's semiconductor nature. The above results show that the NZC ferrite thinfilm is highly suitable for gas sensing applications.

Author Contributions

All authors examined the findings and approved the final manuscript version.

Acknowledgement

The authors would like to thank the IIT Bombay Nanofabrication Facility (IITBNF) and the Indian Nanoelectronics User Programme (INUP) for supporting this research under project ID: RD/0121-MEITY01-002 INUP i2i. This study got no specific financing from public, commercial, or non-profit organisations.

References

[1] Pratibha Rao et al., "Ferrite Thin Films: Synthesis, Characterization and Gas Sensing Properties towards LPG," *Materials Chemistry and Physics*, vol. 149-150, pp. 333-338, 2015. [CrossRef] [Google Scholar] [Publisher Link]

[2] Salah Abdul-Jabbar Jassim, Abubaker A. Rashid Ali Zumaila, and Gassan Abdella Ali Al Waly, "Influence of Substrate Temperature on the Structural, Optical and Electrical Properties of CDS Thin Films Deposited by Thermal Evaporation," *Results in Physics*, vol. 3, pp. 173–178, 2013. [CrossRef] [Google Scholar] [Publisher Link]

[3] Amir Masoud Soleimanpour, and Ahalapitiya H. Jayatissa, "Characterization of Porous Nickel Oxide Base Hydrogen Gas Sensor," *International Semiconductor Device Research Symposium*, pp. 1-2, 2011. [CrossRef] [Google Scholar] [Publisher Link]

[4] Ahmed Belahmar, and Ali Chouiyakh, "Effect of Substrate Temperature on Structural and Optical Properties of Au/SiO2 Nanocomposite Films Prepared by RF Magnetron Sputtering," *Open Access Library Journal*, vol. 4, no. 8, 2017. [CrossRef] [Google Scholar] [Publisher Link]

[5] G. Eranna et al., "Oxide Materials for Development of Integrated Gas Sensors—A Comprehensive Review," *Critical Reviews in Solid State and Materials Sciences*, vol. 29, no. 3-4, pp. 111-188, 2010. [CrossRef] [Google Scholar] [Publisher Link]

[6] S. S. Kumbhara et al., "Synthesis and Characterization of Spray Deposited Nickel-Zinc Ferrite Thin Films," *Energy Procedia*, vol. 54, pp. 599–605, 2014. [CrossRef] [Google Scholar] [Publisher Link]

[7] Saptarshi De, "Fast Response of Pulsed Laser Deposited Zinc Ferrite Thin Film as a Chemo-Resistive Gas Sensor," *Arxiv preprint Applied Physics*, 2019. [CrossRef] [Google Scholar] [Publisher Link]

[8] L. Fkhar et al., "Cobalt Substitution Effect on the Structure and Magnetic Proprieties of Fe3O4 Nano-Particles," *Advances in Materials and Processing Technologies*, vol. 8, no. 1, pp. 401-407, 2020. [CrossRef] [Google Scholar] [Publisher Link]

[9] Zainab T. Hussain et al., "Investigating the Effect of Aluminum dopping on the Structural, Optical, Electrical, and Sensing Properties of ZnO Films," *Advances in Materials and Processing Technologies*, vol. 8, no. 2, pp. 1715-1727, 2022. [CrossRef] [Google Scholar] [Publisher Link]

[10] Shampa Mondal, "LPG Sensing Property of Nickel Doped CDS Thin Film Synthesised by Silar Method," *Advances in Materials and Processing Technologies*, vol. 8, no. 1, pp. 344-354, 2020. [CrossRef] [Google Scholar] [Publisher Link]

[11] S. B. Madake et al., "The Influence of Nickel Substitution on the Structural and Gas Sensing Properties of Sprayed ZnFe2O4 Thin Films," *Journal of Materials Science: Materials in Electronics*, vol. 33, pp. 6273-6282, 2022. [CrossRef] [Google Scholar] [Publisher Link]

[12] Archana Singh et al., "Preparation and Characterization of Nanocrystalline Nickel Ferrite Thin Films for Development of a Gas Sensor at Room Temperature," *Journal of Materials Science: Materials in Electronics*, vol. 27, pp. 8047-8054, 2016. [CrossRef] [Google Scholar] [Publisher Link]

[13] Yudong Li, Zhenyu Yuan, and Fanli Meng, "Spinel-Type Materials Used for Gas Sensing: A Review," *Sensors*, vol. 20, no. 18, 2020. [CrossRef] [Google Scholar] [Publisher Link]

[14] H. Baqiah et al., "Effects of Aging Time on Microstructure, Hydrophobic and Optical Properties of BiFeO3 Thin Films Synthesized via Sol-Gel Method," *Journal of Ceramic Science and Technology*, vol. 9, no. 4, pp. 419-426, 2019. [CrossRef] [Google Scholar] [Publisher Link]

[15] Savita Vasantrao Thakare, "The Influence of Calcination Temperature on the Formation of Nickel Oxide Nanoparticles by Sol-gel Method," *SSRG International Journal of Applied Chemistry*, vol. 8, no. 1, pp. 26-29, 2021. [CrossRef] [Publisher Link]

[16] E. M. Elsayed et al., "The Effect of Solution pH on the Electrochemical Performance of Nanocrystalline Metal Ferrites MFe2O4 (M=Cu, Zn, and Ni) Thin Films," *Applied Nanoscience*, vol. 6, pp. 485–494, 2016. [CrossRef] [Google Scholar] [Publisher Link]

[17] LIU Feng et al., "Magnetic Properties of NiCuZn Ferrite Thin Films Prepared by the Sol-gel Method," *Journal of Wuhan University of Technology-Materials Science Education*, vol. 22, pp. 506-509, 2007. [CrossRef] [Google Scholar] [Publisher Link]

[18] M. Mónica Guraya et al., "Ni Nanoparticles Dispersed on γ-Al2O3 by Induced-Gelation Sol-Gel Method," *SSRG International Journal of Applied Chemistry*, vol. 3, no. 2, pp. 1-8, 2016. [CrossRef] [Google Scholar] [Publisher Link]

[19] Gagan Dixit et al., "Structural, Magnetic and Optical Studies of Nickel Ferrite Thin Films," *Advanced Materials Letters*, vol. 3, no. 1, pp. 21-28, 2012. [CrossRef] [Google Scholar] [Publisher Link]

[20] O. F. Caltun, "Pulsed Laser Deposition of Ni-Zn Ferrite Thin Films," *Journal of Optoelectronics and Advanced Materials*, vol. 7, no. 2, pp. 739–744, 2005. [Google Scholar] [Publisher Link]

[21] Farhana Naaz et al., "Structural and Magnetic Properties of MgFe2O4 Nanopowder Synthesized via Co-Precipitation Route," *SN Applied Sciences*, vol. 2, no. 808, 2020. [CrossRef] [Google Scholar] [Publisher Link]

[22] R. Madhusudhana, R. Gopalakrishne Urs, and L. Krishnamurthy, "ZrO2-TiO2 Multi-Layered Nanostructured Coatings on AA5052 Substrate as Corrosion and Thermal Barrier Coatings," *SSRG International Journal of Material Science and Engineering*, vol. 8, no. 3, pp. 1-5, 2022. [CrossRef] [Publisher Link]

[23] J.H. Yin et al., "Magnetic Properties of Co-Ferrite Thin Films Prepared by PLD with in Situ Heating and Post-Annealing," *Journal of Magnetism and Magnetic Materials*, vol. 303, no. 2, pp. e387–e391, 2006. [CrossRef] [Google Scholar] [Publisher Link]

[24] G.S. Shahane et al., "Synthesis and Characterization of Ni–Zn Ferrite Nanoparticles," *Journal of Magnetism and Magnetic Materials*, vol. 322, no. 8, pp. 1015–1019, 2010. [CrossRef] [Google Scholar] [Publisher Link]

[25] V. Manikandan et al., "Effect of Temperature on Gas Sensing Properties of Lithium Substituted $NiFe_2O4$ Nickel Ferrite Thin Film," *Journal of Molecular Structure*, vol. 1177, pp. 485-490, 2019. [CrossRef] [Google Scholar] [Publisher Link]

[26] Yue Wu, and Hongxing Zheng, "Modeling of Ferrite Thin-Film Structure using FDTD Method in Optoelectronic Devices," *Proceedings 10th International Symposium on Advanced Optical Manufacturing and Testing Technologies: Novel Optoelectronic Functional Materials and Devices*, vol. 12074, 2021. [CrossRef] [Google Scholar] [Publisher Link]

[27] Shauna Robbennolt et al., "Fabrication and Magnetic Properties of Sol-Gel derived NiZn Ferrite Thin Films for Microwave Applications," *Advanced Materials Letters*, vol. 9, no. 5, pp. 345-352, 2018. [CrossRef] [Google Scholar] [Publisher Link]

[28] Ming-ShienYen, "Hydrothermal Synthesis of Zirconia/Silica Hybrid Materials and their Application on Cotton Fabrics," *SSRG International Journal of Applied Chemistry*, vol. 7, no. 2, pp. 56-62, 2020. [CrossRef] [Publisher Link]

[29] Tao Yuan et al., "The Microstructure and Magnetic Properties of Ni0.4Zn0.6Fe2O4 Films Prepared by Spincoating Method," *Journal of Sol-Gel Science and Technology*, vol. 58, pp. 501-506, 2011. [CrossRef] [Google Scholar] [Publisher Link]

[30] G. Caruntu et al., "Synthesis and Characterization of Ferrite Thin Films Obtained by Soft Chemical Methods," *Tech Connect Briefs*, vol. 3, pp. 338-341, 2004. [Google Scholar] [Publisher Link]